Optimal Model Predictive Controller for Grid-Connected Voltage Source Converters

Mardani, Mohammad Mehdi; Mijatovic, Nenad; Dragicevic, Tomislav

Link back to DTU Orbit

Optimal Model Predictive Controller for Grid-Connected Voltage Source Converters

1st Mohammad Mehdi Mardani
Department of Electrical Engineering
Technical University of Denmark (DTU)
Copenhagen, Denmark.
Sino-Danish College (SDC)
University of Chinese Academy of Sciences
mmema@elektro.dtu.dk

2nd Nenad Mijatovic
Department of Electrical Engineering
Technical University of Denmark (DTU)
Copenhagen, Denmark.
nm@elektro.dtu.dk

3rd Tomislav Dragicevic
Department of Electrical Engineering
Technical University of Denmark (DTU)
Copenhagen, Denmark.
tomdr@elektro.dtu.dk

Abstract—**Grid-connected power electronic converters are the fundamental building blocks of future power electronic-based power systems. Their fast dynamic performance and robustness are the key requirements for ensuring the reliable operation of such systems. This letter proposes a simple optimal model predictive controller (MPC) to control the active and the reactive current of the three-phase voltage source grid-connected converters. Better performance over other state-of-the-art controllers is evaluated based on quantitative criteria comprising the settling time, and the percentage of the overshoot. Finally, the experimental tests are provided to prove the applicability of the proposed approach.**

Index Terms—**Model predictive control (MPC), optimal performance, voltage source converter (VSC), current control, distributed power generation**

I. Introduction

Grid-connected converters, especially voltage source converters (VSCs), are the key building blocks of the future power-electronic-based power grids. VSCs are employed as interfaces between the alternating current (ac) legacy grid and direct current (dc)-based renewable resources such as PV, wind, energy storage systems, and modern loads such as electric vehicle chargers. Due to high presence of VSCs and consequently their significant impact on the grid, it is highly desirable to maximize the dynamic performance of each one of them [1].

Currently, depending on the operational mode, the grid-tied VSCs are usually divided into grid following, grid supporting, and grid forming converters [2], [3]. For any mode of operation, inner current control is an inevitable control structure. The most common current control approach is utilizing linear controllers [4]. Among linear controllers, PI controllers, deployed in the synchronous reference frame, or PR controllers, deployed in stationary reference frames, are widely accepted in practice [5]. However, these linear controllers suffer from several theoretical and practical drawbacks. For instance, since their control parameters have significant effects on the stability of the overall system, the problem of tuning requires careful consideration. Secondly, the PI controllers can guarantee the performance of the system only around a small vicinity of the equilibrium point. Thirdly, the linear controllers are not

able to improve both settling time and percentage of overshoot simultaneously [6].

Several alternatives current control approaches have been proposed to avoid these drawbacks. An overview on table-based direct power control (DPC) for grid-connected converters was addressed in [7]. For implementing DPC strategies, a lookup switching table is usually predefined. Based on the output angular position and also the instantaneous active and reactive power of the VSC, the optimal switching state is chosen from the table. However, firstly, a high sampling frequency is required to obtain satisfactory performance. Secondly, the switching frequency in this control structure is varying, which may complicate the design procedure of the harmonic filter [7]. The sliding mode control (SMC) [8] and the passivity-based control (PBC) [9] have been largely reported for grid-connected VSCs to obtain a robust performance against system uncertainty in comparison with the lookup table DPC and reach faster transient response than the PI controllers. However, PBC and SMC approaches may result in large ripples, which usually come from their control structure, in both active and reactive power. Additionally, due to the time derivatives, the SMC controllers may result in high sensitivity. Each approach for chattering reduction in SMC, which is designed for power electronic converters, has its advantages and disadvantages [8]. For instance, while the implementation of the SMC-hysteresis function approach is easy, the switching frequency is time-varying and there is a steady-state error if the structure of the hysteresis function is not selected precisely. The SMC-boundary layer approach solves the varying switching frequency, however, there is still a steady-state problem if the bounds of the saturation function are not selected properly. The SMC-state observer approach provides more flexibility, however, it has complicated implementation and requires a lot of effort for designing a controller [8]. The grid voltage modulated (GVM)-DPC is introduced to improve the steady-state performance and robust performance of the grid-connected VSCs than SMC and DPC methods [10]. However, there is no formal analysis for clarifying why and how this is achieved. Ref. [11] uses artificial neural network (ANN) to control a grid-connected VSC.

Although ANN is computationally efficient and can provide close to optimal solutions, its optimality can not be formally proved. The problem of designing fuzzy logic control (FLC) for VSC is addressed in [12]. The advantages of FLC can be enumerated as its efficient, non-model-based structure, and it is adjustable for both linear and nonlinear systems. However, this controller is designed based on trial and error and it has a complex control structure. Ref. [13] investigates the problem of analyzing and designing a nonlinear controller for VSCs. In [13], a feedback linearization method is used to regulate the active power. However, the main drawback of the feedback linearization approach is utilizing nonlinearity cancelation, which may result in poor robust performance. Additionally, many optimization-based methods such as genetic algorithm (GA), particle swarm optimization (PSO), backtracking search optimization algorithm (BSA), and lightning search algorithm (LSA) are presented in the literature to improve the robustness and design a precise controller for VSC [14]. However, these types of controllers are complex with high computing time and require many iterations.

More recently, designing the model predictive control (MPC) for VSCs has received significant attention. The main advantages of MPC are the ability to regulate multi-input-multi-output (MIMO) systems, handle hard constraints, and explicitly account for the nonlinear dynamics as well. In the power electronics control field, the MPC is mainly split into two main categories. The first one is the finite control set (FCS)-MPC and the second one is the continuous control set (CCS)-MPC. In FCS-MPC, the goal is to find an optimal solution of the cost function. In particular, a model is used to predict the system behavior for every possible power converter's switching state and then the best switching state is chosen online [15]. However, by increasing the number of switching states or lengthening the horizon, the number of possible selections exponentially increases, and may become prohibitively computationally heavy for online execution. Additionally, the switching frequency of the FCS-MPC is varying and may cause grid resonances [16]. In clear contrast to the FCS-MPC approaches, the CCS-MPC approach, provides significant advantages such as fixed switching frequency and analytical design procedure [17], [18]. The most common CCS-MPC methods for grid-connected VSCs are generalized predictive control (GPC) [19] and explicit MPC (EMPC) [20]. However, the main drawback with GPC and EMPC strategies is complex formulation. Ref. [18] investigates the problem of designing sensorless CCS-MPC for grid-connected inverters. However, solving linear matrix inequalities (LMIs) in each iteration of the MPC algorithm needs a lot of computational effort. Moreover, the approach [18] is also not fast enough to handle long horizons.

This letter proposes an optimal CCS-MPC as an alternative to conventional current control methods to cope with the control challenges in three-phase grid-connected VSCs. The key contributions of the proposed approach in comparison with the state-of-the-art ones can be enumerated as follows: Firstly, the main issue with MPC is the computational burden
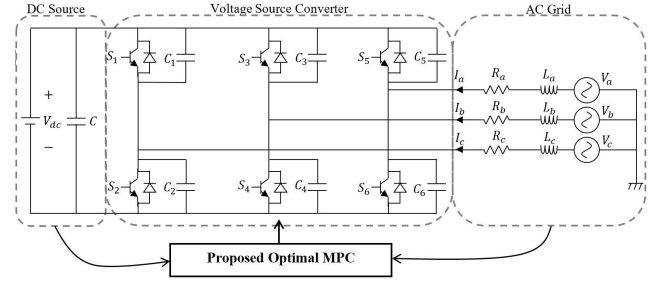

Fig. 1. Three-phase grid-connected VSC.

of the controller. To overcome this issue, this letter proposes a simple CCS-MPC with a long predefined horizon N that is computationally light and can easily be implemented online on a cheap commercial microprocessor. Secondly, the optimal solution for the cost function is obtained through the analytical design procedure. Thus, the designed controller has the fastest possible transient response, which means the lowest settling time and suitable percentage of the overshoot. To validate the practical applicability of the proposed approach, experimental tests are presented, where the results are experimentally compared with the results from other conventional controllers. The rest of this letter is organized as follows: The preliminaries and main results are presented in Section II. In Section III, the proposed approach is experimentally tested and compared with the conventional control approaches. Finally, the conclusion is presented in Section IV.

Notation: The following notation is used in this letter. R^n and $R^{n \times m}$ show the n-dimensional vectors and $n \times m$ matrices, respectively. The n-dimensional identity matrices are denoted by I^n.

II. PRELIMINARIES AND MAIN RESULTS

The three-phase grid-connected VSC is illustrated in Fig. 1, where V_a, V_b, and V_c are three-phase grid input voltages; I_a, I_b, and I_c denote three-phase grid input currents; V_{dc} and C show the constant dc voltage and dc-link capacitor, respectively. $L_a = L_b = L_c = L$ and $R_a = R_b = R_c = R$ denote three-phase inductor and resistance, respectively. $S_1 - S_6$ are the switches of the converters. The three-phase bridge is defined for the switching function in each leg, which defines the ON-OFF status of the converter main switches. S_a, S_b, and S_c denote the switching function of each leg. For a specific instance, $S_a = 1$ means S_1 is ON and S_2 is OFF and also $S_a = 0$ means S_1 is OFF and S_2 is ON. S_b and S_c operate similar to the S_a. In the three-phase abc stationary coordinate, the state space model of the three-phase VSC can be represented as follows:

$$\begin{cases} L\frac{dI_a}{dt} = V_a - RI_a - \frac{2S_a - S_b - S_c}{3}V_{dc} \\ L\frac{dI_b}{dt} = V_b - RI_b - \frac{2S_b - S_a - S_c}{3}V_{dc} \\ L\frac{dI_c}{dt} = V_c - RI_c - \frac{2S_c - S_a - S_b}{3}V_{dc} \end{cases} \quad (1)$$

The equation (1) can be represented as the following equation by employing dq synchronous rotating coordinate transfer:

$$\begin{cases} L\frac{dI_d}{dt} = V_d - RI_d + \omega L I_q - S_d V_{dc} \\ L\frac{dI_q}{dt} = V_q - RI_q - \omega L I_d - S_q V_{dc} \end{cases} \quad (2)$$

where I_d and I_q are active and reactive current in the dq coordinate system, respectively. V_d and V_q denote the active and the reactive voltage in the dq coordinate system, respectively. The angular frequency of the input voltage is denoted by ω, which can be calculated by $\omega = 2\pi f$. Furthermore, the switching functions are denoted by S_d and S_q. Model (2) is used to propose a simple high-performance controller. The equation (2) could be represented as

$$\dot{x} = \begin{bmatrix} -\frac{R}{L} & \omega \\ -\omega & -\frac{R}{L} \end{bmatrix} x + \begin{bmatrix} \frac{1}{L} & 0 \\ 0 & \frac{1}{L} \end{bmatrix} u \quad (3)$$

where $x = \begin{bmatrix} I_d & I_q \end{bmatrix}^T$, and $u = \begin{bmatrix} u_d & u_q \end{bmatrix}^T = \begin{bmatrix} V_d - S_d V_{dc}, V_q - S_q V_{dc} \end{bmatrix}^T$. Using the Euler discretization method, one has

$$\begin{cases} x_k = Ax_{k-1} + Bu_{k-1} \\ yk = Cx_k \end{cases} \quad (4)$$

where $y_k \in R^2$ denotes the discrete-time output variable, which is equal to the state variable in this case. $x_k \in R^2$ is the discrete-time state variable. Known constant matrices $A \in R^{2\times 2}$, $B \in R^{2\times 2}$, and $C = I^2$ are system matrices. The output variables can be predicted as follows:

$$\begin{cases} y(k+1) = CAx(k) + CBu(k) \\ y(k+2) = CA^2x(k) + CABu(k) + CBu(k+1) \\ y(k+N) = CA^N x(k) + \sum_{j=1}^{N} CA^{N-j}Bu(k+j-1) \end{cases} \quad (5)$$

The equation (5) can be represented as follows:

$$Y(k) = Fx(k) + GU(k) \quad (6)$$

where $Y = \begin{bmatrix} y(k+1) \\ y(k+2) \\ y(k+N) \end{bmatrix}$, $U = \begin{bmatrix} u(k) \\ u(k+1) \\ u(k+N) \end{bmatrix}$, $F = \begin{bmatrix} CA \\ CA^2 \\ CA^N \end{bmatrix}$,

and $G = \begin{bmatrix} CB & 0 & \cdots & 0 \\ CAB & CB & 0 & 0 \\ \vdots & \vdots & & \cdots \\ CA^{N-1}B & CA^{N-2}B & \cdots & CB \end{bmatrix}$. The cornerstone of all of the MPC approaches is defining a cost function. Here, the cost function is defined such that it covers a prediction of N horizon and also tracking the reference signal not only for the current time step but also for N horizon ahead. Here, we propose the following cost function for the state-space model (2):

$$J = (Y(k) - W(k))^T P(Y(k) - W(k)) + U^T(k)QU(k) \quad (7)$$

where $W(k)$ is a vector of the reference signals for N future horizon. P and Q are positive definite weighting matrices with suitable dimensions. These matrices can give a relative importance to each variable or the relation between one variable

with another. Additionally, this cost function is essential for making dimensionless state variables (i.e. compensating the large differences in the order of the magnitude of the state variables). The following theorem is presented to find the optimal control signal by minimizing the cost function (7).

Theorem 1 (MPC): For each iteration, the optimal solution for the cost function (7) can be analytically calculated as follows:

$$\min_{U(k)} J \to U(k) = (Q + G^T PG)^{-1}G^T P(W(k) - Fx) \quad (8)$$

Whereas the receding horizon strategy is employed, the first two rows of the $U(k)$ denote the control signal $u(k)$ and implemented to the VSC. Additionally, the switching function is

$$\begin{bmatrix} S_d & S_q \end{bmatrix}^T = \begin{bmatrix} (V_d - u_d)/V_dc & (V_q - u_q)/V_dc \end{bmatrix}^T \quad (9)$$

Proof. Substitute (6) into cost function (7), one has

$$J = ((Fx(k) + GU(k)) - W(k))^T P((Fx(k) + GU(k)) - W(k)) + U^T(k)QU(k) \quad (10)$$

Minimize J with respect to $U(k)$ concludes

$$\frac{\partial J}{\partial U} = G^T P(Fx(k) - W(k)) + (Q + G^T PG)U(k) = 0 \quad (11)$$

By simplifying (11), the proof is completed.

III. EXPERIMENTAL VERIFICATION AND COMPARISON

Fig. 2 illustrates the overall configuration of the experimental setup and the implementation of the proposed optimal MPC on the three-phase VSC. In this experimental test, a personal computer with specification and configuration of core $i5$, 3.4 GHz, $16Gb$ RAM is employed. The proposed optimal MPC control law is simulated by Matlab/Simulink and then experimentally implemented on the prototyping platform dSpace RTI1006. The DS2004 high-speed A/D board is used to digitalize analog input signals, which are the measured DC voltage, three-phase line-to-line voltages, and three-phase currents, of the dSpace with high sample rates. The DS5101 board is employed to generate a multitude of signals at various frequencies including incremental encoder signals and pulse width modulator (PWM) waveform, which are obtained from dSpace. The system consists of a three-phase SPITZENBERGER SPIES supply simulation system to simulate the ac voltage source, a bi-directional power supply to apply DC voltage, an L filter, and a VSC, which is working as an inverter. Each inductance in the L filter is $4.4mH$, which is obtained by a series connection of two separate $2.2mH$ inductances. The series resistance is 0.5Ω.

Fig. 3 and Fig. 4 illustrate the implementation results of the proposed approach and the PI control method on a three-phase VSC setup, respectively. In Fig. 3 (a) and Fig. 4 (a), the blue lines show the ac voltage of one of the three phases. The three-phase currents are illustrated by the red, green, and yellow colors. By comparing Fig. 3 (a) with Fig. 4 (a), one can observe that the proposed approach not only guarantees the fixed

(a)

(b)

Fig. 2. The Laboratory prototype. The configuration of the experimental setup and Implementation of grid-connected VSC with LCL filter.

Fig. 3. Experimental validation for the proposed MPC approach. (a) The ac voltage of one of the three-phase is illustrated by the blue line and the three-phase current of the converter side is shown by red, green, and yellow colors. (b) the red and blue lines show active and reactive currents, respectively.

switching frequency but also that the dynamic performance of the proposed approach is significantly improved in comparison with the state-of-the-art methods. By comparing Fig. 3 (a) with Fig. 4 (a), one can conclude not only the settling time but also the percentage of the overshoot for the proposed approach is significantly better. In start contrast, the PI controller cannot minimize both the settling and percentage of the overshoot together. Additionally, tuning and designing the controller parameters of the PI controller need significant effort, however, designing the proposed MPC controller is much simpler than the PI controller. The behavior of the active and reactive current for both the proposed approach and PI controller are shown in Fig. 3 (b) and Fig. 4 (b), respectively. The same discussion regarding transient and steady-state conditions is satisfied for active and reactive current as well.

IV. CONCLUSIONS

This letter proposed a new CCS-MPC method for current control of three-phase grid-tied VSCs. Due to the simple structure of the controller besides the advanced method, there was no complexity and computational issue even for the long horizon of the MPC. The theoretical and experimental results show that active and reactive current are controlled in optimal way, where not only the settling time but also the percentage of overshoot is optimized. Furthermore, when comparted to the FCS-MPC, the frequency switching of the proposed approach is constant. In comparison with the conventional PI controllers, the experimental results illustrated the better performance and applicability of the proposed approach.

REFERENCES

[1] T. Dragičević, "Model predictive control of power converters for robust and fast operation of ac microgrids," *IEEE Transactions on Power Electronics*, vol. 33, no. 7, pp. 6304–6317, 2017.

[2] M. G. Taul, C. Wu, S.-F. Chou, and F. Blaabjerg, "Optimal controller design for transient stability enhancement of grid-following converters under weak-grid conditions," *IEEE Transactions on Power Electronics*, vol. 36, no. 9, pp. 10 251–10 264, 2021.

[3] T. Dragičević, S. Vazquez, and P. Wheeler, "Advanced control methods for power converters in distributed generation systems and microgrids," *IEEE Transactions on Industrial Electronics*, vol. 66, no. 11, pp. 8866–8869, 2019.

[4] K. Sun, W. Yao, J. Fang, X. Ai, J. Wen, and S. Cheng, "Impedance modeling and stability analysis of grid-connected dfig-based wind farm with a vsc-hvdc," *IEEE Journal of Emerging and Selected Topics in Power Electronics*, vol. 8, no. 2, pp. 1375–1390, 2019.

[5] D. N. Zmood and D. G. Holmes, "Stationary frame current regulation of pwm inverters with zero steady-state error," *IEEE Transactions on power electronics*, vol. 18, no. 3, pp. 814–822, 2003.

[6] M. M. Mardani, N. Vafamand, M. H. Khooban, T. Dragičević, and F. Blaabjerg, "Design of quadratic d-stable fuzzy controller for dc micro-grids with multiple cpls," *IEEE Transactions on Industrial Electronics*, vol. 66, no. 6, pp. 4805–4812, 2018.

[7] S. S. Lee and Y. E. Heng, "Table-based dpc for grid connected vsc under unbalanced and distorted grid voltages: Review and optimal method," *Renewable and Sustainable Energy Reviews*, vol. 76, pp. 51–61, 2017.

[8] H. Komurcugil, S. Biricik, S. Bayhan, and Z. Zhang, "Sliding mode control: Overview of its applications in power converters," *IEEE Industrial Electronics Magazine*, vol. 15, no. 1, pp. 40–49, 2021.

(a)

(b)

Fig. 4. Experimental validation for the PI controller. (a) The ac voltage of one of the three-phase is illustrated by the blue line and the three-phase current of the converter side. (b) the red and blue lines show active and reactive currents, respectively.

[9] D. del Puerto-Flores, J. M. Scherpen, M. Liserre, M. M. de Vries, M. J. Kransse, and V. G. Monopoli, "Passivity-based control by series/parallel

[16] X. Guo, H.-P. Ren, and J. Li, "Robust model-predictive control for a compound active-clamp three-phase soft-switching pfc converter under damping of single-phase pwm voltage source converter," *IEEE Transactions on Control Systems Technology*, vol. 22, no. 4, pp. 1310–1322, 2013.

[10] Y. Gui, X. Wang, F. Blaabjerg, and D. Pan, "Control of grid-connected voltage-source converters: The relationship between direct-power control and vector-current control," *IEEE Industrial Electronics Magazine*, vol. 13, no. 2, pp. 31–40, 2019.

[11] S. Li, M. Fairbank, C. Johnson, D. C. Wunsch, E. Alonso, and J. L. Proao, "Artificial neural networks for control of a grid-connected recti-fier/inverter under disturbance, dynamic and power converter switching conditions," *IEEE transactions on neural networks and learning systems*, vol. 25, no. 4, pp. 738–750, 2013.

[12] M. A. Hannan, Z. A. Ghani, M. M. Hoque, P. J. Ker, A. Hussain, and A. Mohamed, "Fuzzy logic inverter controller in photovoltaic applications: Issues and recommendations," *IEEE Access*, vol. 7, pp. 24 934–24 955, 2019.

[13] J. Khazaei, Z. Tu, A. Asrari, and W. Liu, "Feedback linearization control of converters with lcl filter for weak ac grid integration," *IEEE Transactions on Power Systems*, vol. 38, no. 4, pp. 3740–3750, 2021.

[14] M. Hannan, J. A. Ali, A. Mohamed, and A. Hussain, "Optimization techniques to enhance the performance of induction motor drives: A review," *Renewable and Sustainable Energy Reviews*, vol. 81, pp. 1611–1626, 2018.

[15] M. Novak, U. M. Nyman, T. Dragicevic, and F. Blaabjerg, "Statistical model checking for finite-set model predictive control converters: A tutorial on modeling and performance verification," *IEEE Industrial Electronics Magazine*, vol. 13, no. 3, pp. 6–15, 2019.
unbalanced grid condition," *IEEE Transactions on Industrial Electronics*, vol. 65, no. 3, pp. 2156–2166, 2017.

[17] Z. Song, Y. Tian, W. Chen, Z. Zou, and Z. Chen, "Predictive duty cycle control of three-phase active-front-end rectifiers," *IEEE Transactions on Power Electronics*, vol. 31, no. 1, pp. 698–710, 2015.

[18] N. N. N. Nam, N.-D. Nguyen, C. Yoon, M. Choi, and Y. I. Lee, "Voltage sensorless model predictive control for a grid-connected inverter with lcl filter," *IEEE Transactions on Industrial Electronics*, 2021.

[19] M. G. Judewicz, S. A. González, N. I. Echeverría, J. R. Fischer, and D. O. Carrica, "Generalized predictive current control (gpcc) for grid-tie three-phase inverters," *IEEE Transactions on Industrial Electronics*, vol. 63, no. 7, pp. 4475–4484, 2015.

[20] S. Borreggine, V. G. Monopoli, G. Rizzello, D. Naso, F. Cupertino, and R. Consoletti, "A review on model predictive control and its applications in power electronics," in *2019 AEIT International Conference of Electrical and Electronic Technologies for Automotive (AEIT AUTOMOTIVE)*, pp. 1–6. IEEE, 2019.